Analysis of Finite-Precision Adaptive Filters Part II: Computation of the Residual Signal Distribution

Analyse wertdiskreter Adaptionsverfahren Teil II: Berechnung der Restsignal-Verteilung

By Bernd Friedrichs*

Abstract:

Adaptive filters are updated with the stochastic gradient least mean squares algorithm (LMS) in many applications. A generally remaining dithering of the coefficients causes a residual signal with a variance which was calculated in Part I [2].

If adaptive filters are used in digital receivers for data communication, additional information about the statistics of the residual signal would be useful for the calculation of the overall error probability. This contribution deals with the exact computation of the amplitude distribution of the residual signal, both for infinite- as finite-precision adaptive operation. As main result, the residual signal is established as Gaussian distributed even for adaptive filters with only one coefficient, if certain conditions are fulfilled. The widely used assumptions for the analysis of adaptive filtering are partly confirmed and otherwise partly refused.

Übersicht:

Für adaptive Filter wird bei vielen Anwendungen das stochastische Gradientenverfahren (LMS-Algorithmus) zur Einstellung der Koeffizienten verwendet. Ein grundsätzlich immer verbleibendes Zittern der Koeffizienten führt zu einem Restsignal, dessen Varianz in Teil I [2] berechnet wurde.

Beim Einsatz adaptiver Filter in digitalen Empfängern zur Datenübertragung sollten zur Berechnung der Fehlerwahrscheinlichkeit die statistischen Eigenschaften des Restsignals bekannt sein. Die Amplitudenverteilung des Restsignals wird hier sowohl für die wertkontinuierliche wie die wertdiskrete Adaption exakt berechnet. Als Hauptergebnis erweist sich das Restsignal als normalverteilt schon für Filter mit nur einem Koeffizienten, sofern gewisse Voraussetzungen erfüllt sind. Die üblichen Annahmen für die Analyse adaptiver Filter werden teilweise bestätigt und teilweise widerlegt.

Für die Dokumentation:

Adaptive Filter / LMS-Algorithmus / Koeffizientenzittern / Quantisierung / Konvergenz von Verteilungen / Funktionalgleichungen / Differential- und Differenzengleichungen

1. Introduction

Adaptive filters have been introduced and analysed with respect to their second-order statistics in Part I [2]. The coefficient updating is performed with the least mean squares (LMS) algorithm:

$$c_{k+1} = c_k + \alpha a_k Q(u_k + \varphi_k). \tag{1}$$

Even for the converged steady-state, a permanent dithering of the coefficients still remains, i.e. fluctuations around the vector c_{opt} of the optimal settings. Hence, a residual signal $\varphi_k = y_k - \hat{y}_k = a_k^T \varepsilon_k$ remains, where $\varepsilon_k = c_{opt} - c_k$ denotes the misalignment vector. The amount of dithering is measured with the variance of the zero-mean residual signal: $\sigma_k^2 = E(\varphi_k^2)$. The remaining final steady-state error σ_∞^2 has been computed in Part I in dependence on the quantization function Q (Q-LMS). Special cases are sign adaptation (S-LMS) with $Q = \text{sign}$ as the simplest finite-precision implementation and otherwise infinite-precision adaptation (C-LMS).

The task is now the investigation of the distribution of the random variable φ_k. This would be rather simple for fixed coefficient settings, because in this case the statistics of φ_k are determined only through the random vector a_k of the transmitted data. Due to the dithering of the coefficients, however, c_k is to be regarded as a random vector too, and not as a vector of constants. As a consequence, it turns out that the calculation of the distribution of φ_k will succeed only for the converged filter, i.e. for the steady-state as $k \to \infty$. In most applications, fortunately, only the steady-state of the filter is of interest for the calculation of overall error probabilities.

The existence of a limit distribution for φ_k as $k \to \infty$ was already supposed in Part I in order to make the assumption that the shape of the distribution does not change with time. This hypothesis can also be found in [4], using generally Gaussian distributions. In [6, 8] the misalignment vector is shown to converge to a limit distribution, without explicit calculation of this limit distribution. In [3], other references are cited to establish the limit distribution as Gaussian, if certain assumptions are fulfilled. Nevertheless, this is a contradiction to the results presented here (see theorem 1). Only in [7], the limit distribution is exactly proved as Gaussian, however, using the assumption that the signal u_k and the data a_k are Gaussian distributed. The assumption of Gaussian data simplifies the theoretical analysis very much, but this seems not to be a realistic scenario. Therefore, this contribution concentrates on discrete valued data, especially on binary a_k.

* ANT Telecommunications GmbH, Backnang, Germany

It was already mentioned in Part I that the residual signal is Gaussian distributed. But this assumption was explicitly used only for some theoretical examples, particularly for curves (e) and (f) in Fig. 3 of Part I. Apart from those degenerated distributions of the signal u_k, it is sufficient for the analysis and for practical calculations, if the probability density function (PDF) of the residual signal is a slightly shaped (and perhaps sampled) Gaussian PDF. Most often only the low-order moments need to be known, i.e. the specific type of the distribution has no impact at all. The exact shape of the PDF achieves great attention not before computing the overall error probability in a digital data receiver [1].

As main result it is shown in this contribution both for C-LMS as for S-LMS, that the residual signal attains a Gaussian distribution not exactly but approximately with a high degree of accuracy. This statement is valid even for adaptive filters with only one coefficient. After all however, for some degenerated distributions of the signal u_k, it is otherwise shown that the residual signal is not Gaussian distributed.

Important remark: The stochastic process formed by the residual signal is not white, but is highly correlated. In short-time view the residual signal is approximately even constant. However, the distribution of the residual signal to be evaluated in this contribution is based on a long-time consideration. The way how to calculate an overall error probability in a digital receiver by means of this long-time distribution is described in [1].

2. Simplification of the task

With C-LMS, the coefficients as well as the compensation signal $\hat{y}_k$ are continuous valued. Therefore $\varphi_k = y_k - \hat{y}_k$ is also continuous valued regardless of the signal y_k. Leaving out mathematical refinements, this implies the PDF of φ_k as a continuous function, which can be expanded in a Taylor series.

With Q-LMS, $\hat{y}_k$ is quantized with the quantization step size q_c of the coefficients, i.e. the PDF of $\hat{y}_k$ is composed of Dirac delta functions spaced with q_c. If y_k is continuous valued, φ_k is also continuous valued. Otherwise if y_k is discrete valued (e.g. as output of an FIR-filter), the PDF of the residual signal is composed of delta functions with non-equidistant spacing. With $\alpha \to 0$ follows $q_c \to 0$ and therefore the spacing becomes smaller. Thus, it is not amazing that the limit PDF as $\alpha \to 0$ appears as a continuous function.

Hence, in addition to $k \to \infty$ a second limit process $\alpha \to 0$ is considered. Convergence is exactly defined as pointwise convergence of the characteristic functions, i.e. of the Fourier transforms of the PDF's. In reality for $\alpha > 0$, the PDF of the residual signal results as a sampled version of the slightly shaped continuous limit PDF as $\alpha \to 0$.

The continuous limit PDF is of course much easier to handle than the realistic discrete PDF. This method is obviously only meaningful, if the dispersion (i.e. square root of variance) of the residual signal is much greater than the quantization step size of the residual signal. But this condition is usually fulfilled in most applications as it was pointed out in Part I (see (13)).

In the converged steady-state, every coefficient of the adaptive filter is interpreted as a random variable with a time-invariant distribution, i.e. as a stationary stochastic process. It has only to be shown that c_∞ is Gaussian distributed. This is equivalent with the corresponding proof for the misalignment vector $\varepsilon_\infty = c_{\text{opt}} - c_\infty$. Hence, for binary data this implies the residual signal as exactly Gaussian distributed, since the Gaussian distribution is preserved under multiplication with a statistically invariant binary variable (but this does not apply for multilevel coded data) as well as under multiple superposition. For ease of analysis binary data with $a_k \in \{+1, -1\}$ are supposed now.

The more coefficients the adaptive filter consists of, the better the residual signal seems to be Gaussian distributed. Hence, it is sufficient to establish the Gaussian distribution for a filter with only one coefficient. By the way it should be pointed out that a conclusion as follows is wrong: "The coefficient misalignment depends on a large number of gradient estimations and must therefore be Gaussian distributed by the central limit theorem". The mistake in this or similar conclusions based only on intuitive considerations is as follows: All the gradient estimations are weakly statistically correlated, because they depend on the actual value of the coefficient misalignment, which changes only very slowly with time. However, the central limit argument does not apply for statistically dependent variables. Finally, theorem 1 will state that the residual signal is usually not exactly Gaussian distributed.

For an adaptive filter with only one coefficient c_k and the coefficient misalignment $\varepsilon_k = c_{\text{opt}} - c_k$, the residual signal holds as $\varphi_k = a_k \varepsilon_k$ and it results

$$\sigma_k^2 = \mathrm{E}(\varphi_k^2) = \mathrm{E}(\varepsilon_k^2). \tag{2}$$

For abbreviation $\tilde{u}_k := -a_k u_k$ is introduced. The statistical independence of a_k and u_k implies $\tilde{u}_k$ as zero-mean with variance $\mathrm{E}(\tilde{u}_k^2) = \mathrm{E}(u_k^2) = \sigma_u^2$.

3. Infinite-precision algorithm (C-LMS)

3.1 A functional equation and simple conclusions

For an adaptive filter with one coefficient updated with C-LMS, the 1-dimensional deterministic iteration of the coefficient misalignment is formed to yield

$$\begin{aligned} \varepsilon_{k+1} &= \varepsilon_k - \alpha a_k (u_k + a_k \varepsilon_k) \\ &= (1-\alpha)\varepsilon_k + \alpha \tilde{u}_k. \end{aligned} \tag{3}$$

Obviously ε_{k+1} is not influenced by a_{k+1} and therefore these are two statistically independent random variables. Hence, the Independence Theorem [2, (10)] is directly seen to be valid. Consequently ε_k and $\tilde{u}_k$ are statistically independent too.

The last statement implies immediately

$$\sigma_{k+1}^2 = (1-\alpha)^2 \sigma_k^2 + \alpha^2 \sigma_u^2$$

and with $k \to \infty$ follows $(0 < \alpha < 1)$

$$\sigma_\infty^2 = \frac{\alpha}{2-\alpha} \sigma_u^2. \tag{4}$$

The limit distribution of ε_k as $k \to \infty$ is now supposed to exist with a PDF $f_\varepsilon(e)$ and a characteristic function $C_\varepsilon(\chi)$,

whereby the index ∞ is suppressed. The characteristic function is defined as Fourier transform of the PDF:

$$C_\varepsilon(\chi) = \mathrm{E}(\mathrm{e}^{-\mathrm{j}2\pi\chi\varepsilon}) = \int_{-\infty}^{\infty} \mathrm{e}^{-\mathrm{j}2\pi\chi e} f_\varepsilon(e)\,\mathrm{d}e. \tag{5}$$

For a Gaussian distribution applies

$$C_\varepsilon(\chi) = \exp(-2\pi^2\sigma_\infty^2\chi^2).$$

With standardization to unit variance, the characteristic function of $\varepsilon_\mathrm{N} = \varepsilon/\sigma_\infty$ holds as

$$C_{\varepsilon_\mathrm{N}}(\chi) = C_\varepsilon(\chi/\sigma_\infty). \tag{6}$$

According to (3), $(1-\alpha)\varepsilon + \alpha\tilde{u}$ adopts the same distribution as ε itself, i.e. the PDF's satisfy

$$\begin{aligned} f_\varepsilon(e) &= f_{(1-\alpha)\varepsilon+\alpha\tilde{u}}(e) \\ &= f_{(1-\alpha)\varepsilon}(e) * f_{\alpha u}(e). \end{aligned} \tag{7}$$

The convolution of two PDF's corresponds to a linear homogeneous Fredholm integral equation with asymmetric kernel, which is considered no more. From (7) a functional equation of the characteristic functions can be derived:

$$C_\varepsilon(\chi) = C_\varepsilon((1-\alpha)\chi) \cdot C_u(\alpha\chi). \tag{8}$$

In order to get an expression in closed form for the solution it is observed that repeated application of (8) yields

$$C_\varepsilon(\chi) = C_\varepsilon((1-\alpha)^n\chi) \cdot \prod_{i=0}^{n-1} C_u(\alpha(1-\alpha)^i\chi).$$

$C_\varepsilon(\chi)$ is a continuous function with $C_\varepsilon(0) = 1$ and therefore $n \to \infty$ implies

$$C_\varepsilon(\chi) = \prod_{i=0}^{\infty} C_u(\alpha(1-\alpha)^i\chi). \tag{9}$$

A unique solution of the functional equation (8) is guaranteed by $C_\varepsilon(0) = 1$. However, the expression (9) is worthless, since the infinite product can not be calculated explicitly even for very simple functions $C_u(\chi)$. The only exception is the following theorem, which can be proved rather easy because of the typical form of Gaussian characteristic functions [1]:

Theorem 1: The coefficient misalignment ε is Gaussian distributed, if and only if the signal u is Gaussian distributed.

Since u is usually not exactly Gaussian, ε and the residual signal can not be exactly Gaussian too. However, ε is approximately Gaussian which will be the main result of this contribution.

The standardization to unit variance in (8) yields with the aid of (4) and (6):

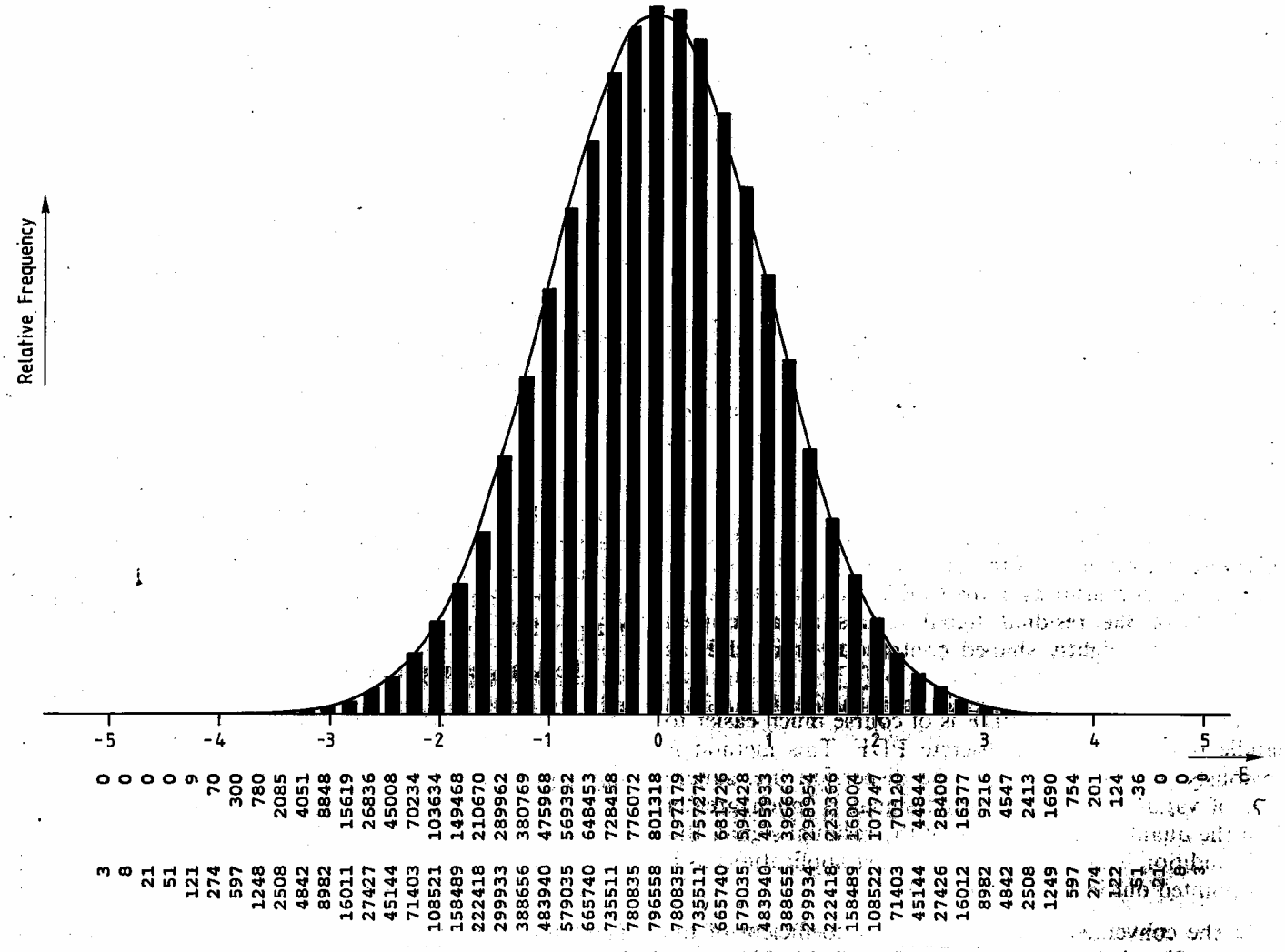

Fig. 1: Histrogram of ε for $\alpha = 0.001$ with C-LMS

$$C_{\varepsilon_N}(\chi) = C_{\varepsilon_N}((1-\alpha)\chi) \cdot C_{u_N}(\sqrt{\alpha(2-\alpha)}\,\chi). \quad (10)$$

This functional equation has a solution depending on α and therefore the limit as $\alpha \to 0$ is of great interest. It should be mentioned that the standardization to unit variance is necessary, because otherwise $\sigma_\infty^2 \to 0$ as $\alpha \to 0$ would only imply the trivial statements $f_\varepsilon(e) \to \delta(e)$ (δ = Dirac delta function) and $C_\varepsilon(\chi) \to 1$.

3.2 Limit distribution of the residual signal as $\alpha \to 0$

Since the type of the distribution of ε depends on α, this dependence will vanish for the limit $\alpha \to 0$ and it is not amazing, that (10) becomes solvable for this limit case. Of course, the solution for this limit case is also of practical importance if the convergence to the limit distribution is sufficiently fast. For this situation the unknown distribution for a specific $\alpha > 0$ can be approximated by the limit distribution as $\alpha \to 0$.

Theorem 2: For small values of α approximately applies

$$C_{\varepsilon_N}(\chi) = \exp\left(\int_0^\chi \frac{C_{u_N}(\sqrt{2\alpha}t) - 1}{\alpha t\, C_{u_N}(\sqrt{2\alpha}t)}\,\mathrm{d}t\right). \quad (11)$$

For any arbitrary distribution of the signal u (included PDF's composed of delta functions), the distribution of ε converges exactly to the Gaussian distribution as $\alpha \to 0$, i.e.

$$\lim_{\alpha \to 0} C_{\varepsilon_N}(\chi) = \exp(-2\pi^2\chi^2). \quad (12)$$

If $\alpha = 0$ is inserted in (10), only the trivial statement $C_{\varepsilon_N}(\chi) = C_{\varepsilon_N}(\chi)\, C_{u_N}(0)$ results. Thus, it is unavoidable to derive (approximately) for (8) an explicit solution given by (11) and then to set $\alpha = 0$ or $\alpha \to 0$ in this solution. The proof is sketched in the appendix.

Fig. 1 shows the result of a simulation over 10^7 cycles for $\alpha = 0.001$. The misalignment ε, standardized to unit variance, is displayed as histogram, which is formed by quantization intervals of width 0.2. Each bar of the histogram is supplied with the numbers of observed samples (upper line) and theoretically expected samples (lower line). The small deviations to the Gaussian distribution are statistically insignificant. The same conformity appears already for $\alpha = 0.1$ showing the very fast convergence to the limit distribution as $\alpha \to 0$.

It should be noted that small values of α require a great amount of simulation time, which is easily to understand: If ε has achieved a large amplitude, then ε remains in this range of large amplitudes for a rather long time, because a small α causes slow changes of ε. Consequently, large amplitudes are not an isolated event but appear during a longer time period. Since large amplitudes are rare in white Gaussian processes, such a long time period is extremly rare in the coloured Gaussian process given by ε. Thus, for a short simulation time, ε would almost never attain larger amplitudes. A great amount of simulation time is hence required to see exactly the convergence to the limit distribution as $\alpha \to 0$.

4. Sign adaptation (S-LMS)

4.1 A functional equation

Similar to (3), the 1-dimensional deterministic iteration of the coefficient misalignment for S-LMS can be written as

$$\begin{aligned}\varepsilon_{k+1} &= \varepsilon_k - \alpha a_k \operatorname{sign}(u_k + a_k \varepsilon_k) \\ &= \varepsilon_k + \alpha \operatorname{sign}(\tilde{u}_k - \varepsilon_k).\end{aligned} \quad (13)$$

The identical distribution of the signals u and $\tilde{u}$ is supposed to be symmetric with a cumulative distribution function denoted by $F_u(\eta) = P(u \le \eta)$. With some calculations [1], a functional equation for f_ε can be derived from (13):

$$f_\varepsilon(e) = F_u(-e+\alpha)\, f_\varepsilon(e-\alpha) + F_u(e+\alpha)\, f_\varepsilon(e+\alpha). \quad (14)$$

The solution depends on α obviously. The direct solution method seems very difficult, because Fourier transformation of (14) yields the characteristic functions, but the multiplications results in a convolution and therefore an integral equation appears. The equation (14) becomes easier to solve only with additional assumptions on the signal u.

4.2 Limit distribution as $\alpha \to 0$ for a continuous valued signal u

It is now supposed that the PDF f_u can be expanded in a Taylor series at point 0. The same statements as in Part I [2] apply for the required accuracy and for the abandonment after low order terms in the series. The Taylor expansion for the cumulative distribution function takes the form

$$F_u(\xi) = \frac{1}{2} + \sum_{r=1}^{\infty} \frac{F_u^{(r)}(0)}{r!}\,\xi^r. \quad (15)$$

The insertion of this series in (14) yields a simplified functional equation, where $f_\varepsilon(e)$ is only weighted with powers of e:

$$f_\varepsilon(e) = \sum_{r=0}^{\infty} \frac{F_u^{(r)}(0)}{r!}\left((-e+\alpha)^r f_\varepsilon(e-\alpha) + (e+\alpha)^r f_\varepsilon(e+\alpha)\right). \quad (16)$$

From (16), a linear differential equation of the characteristic functions of "infinite order" with non-constant coefficients can be derived by means of Fourier transform with the aid of the Fourier correspondence

$$e^r f_\varepsilon(e) \circ\!\!-\!\!\bullet\, (-\mathrm{j}2\pi)^{-r} C_\varepsilon^{(r)}(\chi):$$

$$C_\varepsilon(\chi) = \sum_{r=0}^{\infty} \frac{F_u^{(r)}(0)}{r!(-\mathrm{j}2\pi)^r}\left((-1)^r \mathrm{e}^{-\mathrm{j}2\pi\chi\alpha} + \mathrm{e}^{\mathrm{j}2\pi\chi\alpha}\right) C_\varepsilon^{(r)}(\chi). \quad (17)$$

If the summation is abandoned after $r = 1$, the standardization to unit variance yields a representation as follows:

$$C_{\varepsilon_N}(\chi) = \cos\left(\frac{2\pi\chi\alpha}{\sigma_\infty}\right) C_{\varepsilon_N}(\chi) - \frac{f_{u_N}(0)}{\pi}\,\frac{\sigma_\infty}{\sigma_u}\,\sin\left(\frac{2\pi\chi\alpha}{\sigma_\infty}\right) C'_{\varepsilon_N}(\chi). \quad (18)$$

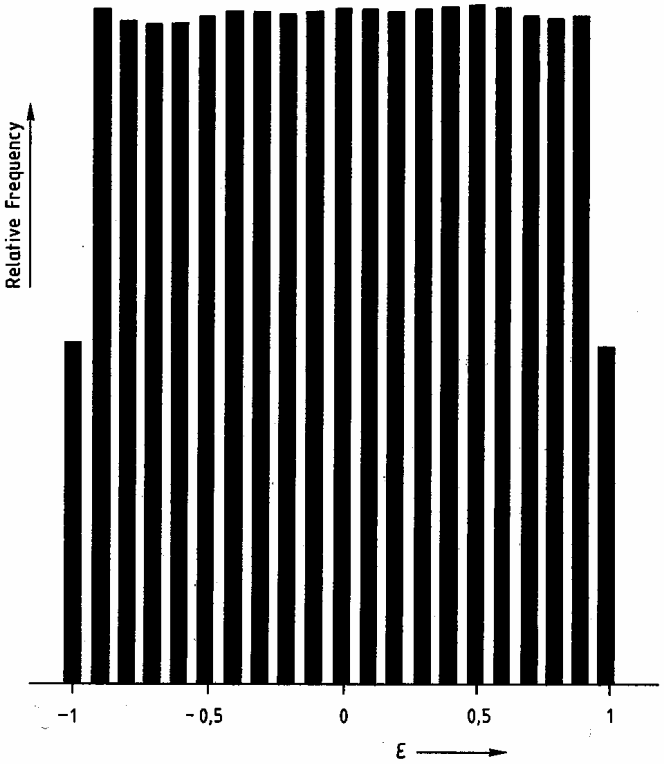

Fig. 2: Histogram of ε for $\alpha = 0.1$ with S-LMS and binary u

The solution of this differential equation for the limit case $\alpha \to 0$ is given by the next theorem, which can be proved with similar methods as theorem 2:

Theorem 3: In case of $f_{u_N}(0) \gg 0$ approximately applies

$$C_{\varepsilon_N}(\chi) = \left[\frac{1+\cos(4\pi\sqrt{f_u(0)\,\alpha}\,\chi)}{2}\right]^{\frac{1}{2f_u(0)\alpha}}. \qquad (19)$$

For any arbitrary PDF satisfying $f_{u_N}(0) \gg 0$, the distribution of the coefficient misalignment converges to the Gaussian distribution as $\alpha \to 0$.

4.3 *Limit distribution as $\alpha \to 0$ for a discrete valued signal u*

The methods presented in the previous subsection for signals with continuous values, of course, are completely unsuitable for signals with discrete values, where the PDF is composed of delta functions. The calculation of the limit distribution is more difficult for the discrete situation and therefore this contribution deals only with the one extreme case of a binary signal u and finally with the other extreme case of a vanishing signal u. For these cases it is possible (and on the other hand also necessary) to compute the PDF of the residual signal in a closed analytical form. This procedure delivers also at first time an exact result for the steady-state error, which was already referred to in [2, Fig. 3].

According to (13), only multiples of α are possible values for ε. Therefore the PDF of ε can be modeled as a sequence of delta functions

$$f_\varepsilon(e) = \sum_{n=-\infty}^{\infty} f_n \cdot \delta(e - n\alpha) \qquad (20)$$

with unknown coefficients f_n (depending on α) satisfying the constraints $\sum_n f_n = 1$ and $f_n = f_{-n}$. With this attempt, the functional equation (14) reduces to a linear difference equation:

$$f_n = F_u(\alpha(1-n))\, f_{n-1} + F_u(\alpha(1+n))\, f_{n+1}. \qquad (21)$$

The first extreme case to be considered is given by a binary signal $u: u \in \{-\sigma_u, +\sigma_u\}$. The lowest integer upper bound of σ_u/α is denoted by m_α. The solution of (21) can be evaluated by elementary but rather extensive operations [1]:

$$f_n = \begin{cases} \dfrac{1}{2m_\alpha} & \text{for } |n| \le m_\alpha - 1 \\ \dfrac{1}{4m_\alpha} & \text{for } |n| = m_\alpha \\ 0 & \text{for } |n| \ge m_\alpha + 1 \end{cases}. \qquad (22)$$

Thus, the distribution of the residual signal is established as a sampled version of a uniform distribution with maximum $\max|\varphi| \approx \sigma_u$. The variance satisfies $\sigma_\infty^2 > \sigma_u^2/3$, i.e. $R_\infty \ge -4.8$ dB. The final steady-state error remains larger than a certain lower bound even for $\alpha \to 0$. **Fig. 2** displays a histogram of ε for $\alpha = 0.1$, resulting from a simulation over 10^6 cycles, showing an excellent agreement with the theoretically evaluated distribution.

By the way, the limit distribution as $\alpha \to 0$ proves to be continuous even for the discrete valued u. The curve (e) from [2, Fig. 3], calculated under the assumption of a Gaussian distributed residual signal, now turns out to be absolutely wrong. Hence, it is approved again, that the usual assumptions and methods suitable for the infinite-precision operation are not automatically applicable for S-LMS or Q-LMS.

The second and last extreme case to be considered is given by an all-zero signal u. Then the difference equation

(21) is easy to solve and ε turns out to be ternary (i.e. the PDF is composed of 3 delta functions). Although the ternary distribution differs very much from the Gaussian distribution, both distributions of the residual signal are resulting in similar variances, i.e. the curve (f) from [2, Fig. 3] can be calculated with the assumption of a Gaussian distribution as well as with knowledge of the exact ternary distribution.

Appendix: Sketch of the proof of theorem 2

Starting point is the Taylor series expansion of $C_{\varepsilon_N}(\chi)$:

$$C_{\varepsilon_N}(\chi-\alpha\chi)=C_{\varepsilon_N}(\chi)-\alpha\chi C'_{\varepsilon_N}(\chi)+R(\chi) \qquad (23)$$

$$\text{with} \quad R(\chi)=\frac{1}{2}\alpha^2\chi^2 C''_{\varepsilon_N}(\chi_0).$$

From $C''_{\varepsilon_N}(\chi_0)=\mathrm{E}((-\mathrm{j}2\pi\varepsilon_N)^2\exp(-\mathrm{j}2\pi\chi_0\varepsilon_N))$ follows $|R(\chi)|\le 2\pi^2\alpha^2\chi^2$. Insertion of (23) in (10) yields

$$C_{\varepsilon_N}(\chi)=(C_{\varepsilon_N}(\chi)-\alpha\chi C'_{\varepsilon_N}(\chi)+R(\chi))\cdot C_{u_N}(\sqrt{\alpha(2-\alpha)}\,\chi).$$

With simple removings, a linear differential equation of first order can be derived:

$$\frac{C'_{\varepsilon_N}(\chi)}{C_{\varepsilon_N}(\chi)}=\frac{C_{u_N}(\sqrt{\alpha(2-\alpha)}\,\chi)-1}{\alpha\chi C_{u_N}(\sqrt{\alpha(2-\alpha)}\,\chi)}+\frac{R(\chi)}{\alpha\chi C_{\varepsilon_N}(\chi)}. \qquad (24)$$

As $\alpha\to 0$, $2-\alpha$ can be approximated by 2 in the left term of the right side. The right term converges to 0, since $R(\chi)$ is bounded by α^2. Hence, an approximated differential equation results

$$\frac{C'_{\varepsilon_N}(\chi)}{C_{\varepsilon_N}(\chi)}=\frac{C_{u_N}(\sqrt{2\alpha}\chi)-1}{\alpha\chi C_{u_N}(\sqrt{2\alpha}\chi)} \qquad (25)$$

with the solution (11). As $\alpha\to 0$, the right term in (25) approaches the value $-4\pi^2\chi$ [1] and this proves (12).

References:

[1] Friedrichs, B.: Ein Beitrag zur Theorie und Anwendung wertdiskreter Adaptionsverfahren in digitalen Empfängern. Doctoral thesis Universität Erlangen-Nürnberg, 1990.
[2] Friedrichs, B.: Analysis of finite-precision adaptive filters – Part I: Computation of the residual signal variance. Frequenz 46 (1992) 9—10, S. 218—223.
[3] Cowan, C. F. N.; Grant, P. M.: Adaptive filters. Englewood Cliffs: Prentice-Hall, 1985.
[4] Claasen, T. A. C. M.; Mecklenbräuker, W. F. G.: Comparison of the convergence of two algorithms for adaptive FIR digital filters. IEEE Trans. Acoust. Speech Signal Process. Vol. 29 (1981) 3, pp. 670—678.
[5] Gersho, A.: Adaptive filtering with binary reinforcement. IEEE Trans. Inform. Theory, Vol. 30 (1984) 2, pp. 191—199.
[6] Bitmead, R. R.: Convergence in distribution of LMS-type adaptive parameter estimates. IEEE Trans. Autom. Control, Vol. 28 (1983) 1, pp. 54—60.
[7] Bershad, N. J.; Qu, L. Z.: On the probability density function of the LMS adaptive filter weights. IEEE Trans. Acoust. Speech Signal Process. Vol. 37 (1989) 1, pp. 43—56.
[8] Farden, D. C.: Stochastic approximation with correlated data. IEEE Trans. Inform. Theory, Vol. 27 (1981) 1, pp. 105—113.

Dr.-Ing. B. Friedrichs, ANT Nachrichtentechnik GmbH, Gerberstr. 33, D-7150 Backnang

(Received on August 12, 1991)

Berechnung und Aufbau von breitbandigen Zirkulatoren (Teil II)

Design and Realization of Wideband Circulators (Part II)

Von Abdel-Messiah Khilla*

Fortsetzung aus Heft 9 – 10/1992

3. Hohlleiter-Y-Zirkulatoren

Hohlleiter-Y-Zirkulatoren bestehen aus einer symmetrischen Hohlleiterverzweigung mit 120°-Symmetrie, in die zentrisch ein meist kreiszylinderförmiger, seltener ein im Querschnitt dreieckförmiger gyrotroper Ferritzylinder eingebracht wird **(Bild 14).**

Aufgrund der gyrotropen Materialeigenschaften des Ferritmaterials kommt es bei geeigneter Wahl des magnetischen Arbeitspunkts des Ferritmaterials zu einem Zirkulatoreffekt, das heißt, wird z.B. am Tor 1 eine Mikrowelle eingespeist, so wird diese im Idealfall vollständig in den am Tor 2 angeschlossenen Wellenleiter gestreut, während Tor 3 entkoppelt ist. Eine entsprechende Aussage gilt bei Einspeisung der Welle an einem anderen Tor.

Erst im Jahr 1959 wurden die Übertragungseigenschaften von Hohlleiter-Y-Zirkulatoren von verschiedenen Autoren [27–30] durch fast ausschließlich experimentelle Untersuchungen angegeben. Durch Verwendung verschiedener Ferritmaterialien und Änderung des Durchmessers des Ferritzylinders sowie der angelegten magnetischen Gleichfeldstärke wurden Zirkulatoren in verschiedenen Frequenzbändern realisiert [31–35].

Butterweck [36] hat 1963 ein vereinfachtes Hohlleiter-Zirkulator-Modell betrachtet, in dem die Wellenleiter durch, verglichen mit der Hohlleiterbreite, sehr schmale Schlitze an den Verzweigungsbereich angekoppelt sind und das einer feldtheoretischen Analyse leicht zugänglich ist. Die Zirkulatorwirkung wird hierbei auf die beiden in azimutaler Richtung umlaufenden $E_{\pm 110}$-Eigenschwingungen im fast vollständig geschlossenen, kreiszylindrischen Hohlraum zurückgeführt; diese haben wegen

* ANT Nachrichtentechnik, Produktbereiche Raumfahrt, Backnang